International Journal of Agriculture and Biosciences 2025 14(2): 315-324.
https://doi.org/10.47278/journal.ijab/2025.002

RESEARCH ARTICLE

eISSN: 2306-3599; pISSN: 2305-6622

Possibilities of Calculation of Convection Heat Transfer inside Built-up Urban Area

A. Savitsky, M. Radkevich*, K. Shipilova and A. Salokhiddinov

"Tashkent Institute of Irrigation and Agricultural Mechanisation Engineers" National Research University, Tashkent, Qari-Niyazova, 39, Uzbekistan
*Corresponding author: m.radkevich@tiiame.uz

ABSTRACT

Accurate modelling of convective heat transfer processes is imperative for the assessment of the urban heat island effect and the development of measures to enhance the urban microclimate. Existing studies predominantly rely on field observations and wind tunnel experiments, while hydrodynamic modelling endeavors often fall short in providing an accurate representation of heat distribution. This paper proposes a solution grounded in the Navier-Stokes equation, employing a synthesis of an evolutionary approach and multi-variable optimization. The GAMS programming language was utilized to facilitate the calculation. The efficacy of the proposed approach was substantiated through the verification of its performance on a test problem pertaining to the occurrence of convective water motion. This demonstrated the approach's capacity to accurately fulfil the water balance. Subsequent to this, the proposed approach was employed to address the convective heat transfer issue in an urban area, leading to the formulation of a model that delineated the temperature distribution around buildings. This model successfully ensured the precise compliance with the laws of conservation of mass and the absence of wave phenomena.

Keywords: Microclimate, Urban heat island, Convective heat transfer, Heat and mass retention, Navier-Stokes equations, Air flow motion.

Article History
Article # 24-1004
Received: 02-Dec-24
Revised: 24-Dec-24
Accepted: 29-Dec-24
Online First: 09-Jan-25

INTRODUCTION

The urban heat island effect, or UHI, is a well-documented phenomenon that has been extensively researched in numerous cities worldwide (Yuan & Bauer, 2007; Blocken et al., 2011; Gagliano et al., 2014; Santamouris, 2014; Minh & Nguyen, 2019). It is characterized by a rise in temperature ranging from 2 to 5°C within urban areas compared to the surrounding rural regions, persisting for several hours daily (Memon et al., 2008; Minh & Nguyen, 2019). Oke (1982) and Luo et al. (2020) observed a temperature disparity of 5 to 10°C, with some studies documenting temperatures as high as 8 to 15°C.

Urban heat islands (UHI) are an increasingly problematic phenomenon in modern cities, particularly in the context of global climate change. In particular, there is an increased load on urban electricity systems due to the increased consumption of electricity by air conditioning (Turhan et al., 2023; Panwar & Jindal, 2024). Consequently, numerous researchers are investigating the causes and processes of urban heat island formation.

The formation of UHI is influenced by various factors, including artificial temperature and humidity, pollutants, and impervious surfaces, as well as thermal radiation in buildings. This subject has been explored by Minh & Nguyen (2019), Minh & Shukurov (2020) and Ismael et al. (2024). Additionally, the relationship between high temperatures on urban surfaces and the high albedo percentages of road and building surfaces has been investigated by several researchers including Yuan & Bauer (2007), Gago et al. (2013), Gagliano et al. (2014), Santamouris (2014), Minh & Nguyen (2019), Awol et al. (2020), and Mehrotra et al. (2020). These studies also examined the relationship between the heat island effect and the basis of urban design, as well as the potential for mitigating the UHI effect through the reflectivity of buildings. The shape (Fan et al., 2019) and orientation (Mohajer et al., 2023) of buildings relative to the sun and to the direction of prevailing winds is also important.

Cite this Article as: Savitsky A, Radkevich M, Shipilova K and Salokhiddinov A, 2025. Possibilities of calculation of convection heat transfer inside built-up urban area. International Journal of Agriculture and Biosciences 14(2): 315-324. https://doi.org/10.47278/journal.ijab/2025.002

A Publication of Unique Scientific Publishers

The formation of UHI is influenced by various factors, including urban motorized transportation. The uninterrupted flow of vehicles results in elevated levels of heat and pollutant emissions. In metropolitan areas characterized by substantial vehicular traffic, the level of heat emitted is notably higher compared to areas with a limited number of automobiles. Studies conducted in major metropolitan areas such as Chicago and New York have demonstrated a positive correlation between concentrated traffic flows and the intensity of UHI. Public transportation, encompassing buses, trolleybuses, and trams, contributes to UHI formation, though to a lesser extent than passenger cars. Conversely, transportation modes such as subways have been shown to reduce overall heat generation by reducing car traffic (Haddad et al., 2015). The development of infrastructure designed for pedestrians and cyclists has been shown to reduce the dependency on private vehicles, thereby contributing to a decrease in the UHI effect. The findings of several studies indicate a correlation between the development of sustainable transport infrastructure and a reduction in the magnitude of urban heat island effects. Mitigation of the UHI effect is increasingly being pursued through the promotion of sustainable urban transport and green infrastructure (Irfeey et al., 2023).

The predominant causes of the heat island effect are generally recognized to be the intricate geometry of streets in the presence of high-rise buildings, which hinders the absorption of solar radiation by building elements and impedes heat exchange; the thermal properties of building and road surfaces enhance heat retention within the metropolis.

The "greenhouse effect" in urban areas is more pronounced due to the presence of a more polluted atmosphere. This effect is expressed more strongly than in rural areas. The effective albedo of the urban system is reduced due to multiple reflection of solar radiation by the surfaces of buildings. This is also caused by the absorption of heat by the walls of buildings. Additionally, evaporative cooling surfaces are reduced by the soil surface or plant crowns. The aforementioned factors lead to uneven heating of the surface and local convective movement of air masses in urban areas. Consequently, these urban areas experience the formation of specific air mass flows, which are often referred to as heat island effects. These flows can either cool heat islands within cities or, at times, lead to an increase in temperatures within these heat islands. However, it is crucial to acknowledge that this analysis merely documents the existing reality and does not offer a comprehensive solution to address the underlying issues (Yuan & Bauer, 2007; Blocken et al., 2011; Minh & Nguyen, 2019).

In such instances, endeavors to enhance the circumstances are comprised of measures that are subjected to recurrent evaluation through a series of observations.The pursuit of solutions is predominantly executed through the reiteration of measures conducted in disparate locations. However, it is evident that each urban heat island possesses distinct characteristics, rendering such an approach to be ineffective in all instances. These methodologies yield a comprehensive overview of the prevailing temperature distribution. Nevertheless, to exert a substantial influence on heat transfer processes within urban environments, mathematical modeling is imperative (Jia et al., 2025). The calculation of thermal convection inside a high-rise urban zone will allow for more accurate determination of the most significant causes of heat islands, enabling the optimization of efforts and resources to prevent excessive heating of high-rise building groups.The efficacy of these measures will be enhanced in terms of both cost and impact. It is important to note that comparisons between heat islands within a single city are only of an evaluative nature, and measures implemented to combat a heat island in one area cannot be directly transferred to another heat island, even within the same city. This is due to the presence of a unique structure of convective transfer for each group of buildings in each area (Nekkanti & Radhakrishnan, 2024).

According to Nottrott et al. (2011), the mechanism of heat transfer in the convective near-wall boundary layer on the leeward vertical wall of a building was studied experimentally. Studies show that the leeward walls of buildings in urban environments are dominated by a regime of turbulent natural convection. This has important implications for the parameterization of convective heat fluxes in urban areas. Building density has a significant influence on convective heat transfer coefficients. In isolated flows, these coefficients change dramatically with increasing density, whereas in the interaction and slip regimes they decrease smoothly with increasing building density (Liu et al., 2015; Awol et al., 2020). The only way to predict thermal convection within groups of buildings is to solve hydrodynamic problems (Blocken et al., 2011; Gagliano et al., 2014).

Computational fluid dynamics (CFD) modeling is frequently employed as a means of devising efficacious strategies for the mitigation of thermal effects. In urban environments, the convective transport of heat is influenced by a variety of factors, including the geometry of buildings, the physical properties of materials, and the prevailing climatic conditions (Donthu et al., 2024). The growing reliance on CFD modeling can be attributed to its ability to visualize and predict the distribution of airflow and temperature in urban areas. A range of software packages, such as ANSYS Fluent and OpenFOAM, are utilized to facilitate CFD modeling, thereby enabling the detailed modeling of both outdoor and indoor environments. In their work, Mirsadeghi et al. (2013) demonstrated the use of these tools to estimate the exterior heat transfer coefficients required for the energy-efficient design of buildings. Convective transport in urban areas has been a subject of study for numerous researchers. For instance, Moediartianto et al. (2018) conducted field and wind tunnel studies, in addition to three-dimensional Reynolds-averaged Navier-Stokes equation analyses, to study the convective heat transfer coefficient of urban roofs (Blocken et al., 2011; Minh & Nguyen, 2019). However, it was found that the accuracy of the results obtained was insufficient for accurate modeling of the urban climate.

The advent of a highly efficient, conservative finite difference scheme for the transfer of matter and thermal energy was not yet in existence. The scheme, which allows the laws of conservation of matter and energy to be accurately followed, was first used in the problem described in this article. The versatility of these tools in modeling different urban configurations renders them invaluable for predicting the impact of architectural decisions on urban thermodynamics. The application of CFD modeling to investigate heat transfer in urban buildings depending on various factors has been considered by numerous authors, including Chung & Choo (2011), Mirsadeghi et al. (2013), and Schrijvers et al. (2018). While CFD offers numerous advantages, including comprehensive insight into airflow and temperature interactions, it is not without its limitations. The reliability of CFD results is contingent upon the quality of the input data and the validation of the model. As Jun Chung and Choo (2011) observe, discrepancies in the input parameters can result in considerable discrepancies in the outcomes.

Researchers have noted the complexity of hydrodynamic modeling of convective heat transfer processes in urban buildings and the lack of sufficiently accurate results (Yuan & Bauer, 2007; Blocken et al., 2011; Gagliano et al., 2014; Minh & Nguyen, 2019). This observation suggests that a universally accepted solution to this problem remains elusive.

The objective of this study is to demonstrate the feasibility and existence of a mathematical model that captures the dynamics of convective heat transfer within urban buildings. This model is formulated using the equations of hydrodynamics, thereby ensuring full compliance with the laws of conservation of moving masses, energy, and heat. The efficiency and simplicity of the method of describing obstacles in the path of air mass movement by means of the interaction of the air flow with a certain virtual additional phase with certain special properties is shown. This solution can serve as a foundation for modeling the microclimate of urban buildings, thereby substantiating urban planning initiatives and establishing zones of climatic comfort.

MATERIALS & METHODS

The calculation of heat transfer by convection is based on the system of Navier-Stokes equations "truncated" to hydrostatics and with the assumption of incompressibility of the moving medium (Marchuk et al., 1975; Marchuk & Kurbatkin, 1978; Marchuk, 1980; Batchelor & Moffat, 1984; Anderson et al., 1990). It is imperative to acknowledge that this "truncation" is implemented to mitigate the occurrence of sound and shock waves. Absent this truncation, numerical analogues of existing shock and sound waves are inevitable during the computational process. The emergence of shock wave analogues can be attributed to rounding errors, the order of approximation by finite-difference analogues of differential operators, and inconsistency during the establishment of initial conditions. The foundation for subsequent calculations is the system of Navier-Stokes equations (1) reduced to hydrostatics (Furukawa et al., 2020; Gao et al., 2021). This system is widely employed in calculations of air and water circulation (Lax & Richtmyer, 1956; Marchuk et al., 1975; Marchuk & Kurbatkin, 1978; Marchuk, 1980).

$$\begin{cases} \frac{\partial V_x}{\partial t} + V_x\frac{\partial V_x}{\partial x} + V_y\frac{\partial V_x}{\partial y} + V_z\frac{\partial V_x}{\partial z} = -\frac{1}{\varrho}\cdot\frac{\partial P}{\partial x} + \nu\cdot\triangle V_x \\ \frac{\partial V_y}{\partial t} + V_x\frac{\partial V_y}{\partial x} + V_y\frac{\partial V_y}{\partial y} + V_z\frac{\partial V_y}{\partial z} = -\frac{1}{\varrho}\cdot\frac{\partial P}{\partial y} + \nu\cdot\triangle V_y \\ P = g\cdot\int_z^{Zp(x,y)} \varrho\cdot\partial z \\ \frac{\partial V_x}{\partial x} + \frac{\partial V_y}{\partial y} + \frac{\partial V_z}{\partial z} \approx 0 \end{cases} \quad (1)$$

Where: V_x, V_y, V_z are components of the velocity vector along the coordinate axes OX, OY, OZ,

P − pressure,

ν − kinematic viscosity,

Zp (x, y) − position of some surface in the calculation of gas motion or position of the free surface of the liquid in the calculation of liquid motion,

z − vertical coordinate,

g − free-fall acceleration,

ϱ − density,

$\triangle = \frac{\partial^2}{(\partial x)^2} + \frac{\partial^2}{(\partial y)^2} + \frac{\partial^2}{(\partial z)^2}$ − the Laplacean differential operator.

Density in such systems is assumed to be weakly variable and that is why we use the approximate equality sign in the incompressibility equation of the medium.

Let us add to the system (1) the equation of conservation of thermal energy (2) (Wei et al., 2021; Ricardo et al., 2024):

$$\frac{\partial T}{\partial t} + V_x\cdot\frac{\partial T}{\partial x} + V_y\cdot\frac{\partial T}{\partial y} + V_z\cdot\frac{\partial T}{\partial z} = \frac{\lambda}{C\cdot\varrho}\cdot\triangle T \quad (2)$$

where: T is the temperature,

λ − heat transfer coefficient,

C − specific heat capacity.

Adding to the system of equations (1) and (2) the equation of state (Marchuk et al., 1975; Roache, 1976; Marchuk & Kurbatkin, 1978; Marchuk, 1980), we close the system with respect to the variables V_x, V_y, V_z, P, T, ϱ

$$\varrho = \Phi(T) \quad (3)$$

Where: *Φ(T)* is a regularity linking the density of the medium and its temperature.

In hydrodynamic calculations, when preparing an approximate solution algorithm, the incompressibility equation (4) is integrated vertically and the obvious fact that in the vertical direction the velocity of the free surface coincides with the vertical velocity of particles lying on this surface is used. The result of such actions is the appearance of the evolutionary equation for determining the position of the free surface (5). Evolutionary equations with respect to some variable are equations in which the first time derivative of this variable is present.

$$\int_{Z_g}^{Z_p}\left(\frac{\partial V_x}{\partial x} + \frac{\partial V_y}{\partial y}\right)\partial z = -\int_{Z_g}^{Z_p}\frac{\partial V_z}{\partial z}\partial z = -V_z|_{z=Z_p} \quad (4)$$

$$\frac{\partial Z_p}{\partial t} + V_x\cdot\frac{\partial Z_p}{\partial x} + V_y\cdot\frac{\partial Z_p}{\partial y} = V_z|_{z=Z_p} \quad (5)$$

Let us substitute into the horizontal components of the equation of motion the hydrostatic pressure:

$$P = g\cdot\int_z^{Zp(x,y)} \varrho\cdot\partial z \quad (6)$$

By application of the Leibniz formula for the differentiation of a definite integral with variable integration limits [8], we obtain system (7):

$$\begin{cases} \frac{\partial V_x}{\partial t} + V_x\frac{\partial V_x}{\partial x} + V_y\frac{\partial V_x}{\partial y} + V_z\frac{\partial V_x}{\partial z} = -\frac{g}{\varrho}\cdot\left(\int_z^{Zp(x,y)}\frac{\partial\varrho(x,z)}{\partial x}\cdot\partial z + \frac{\partial Zp(x,y)}{\partial x}\cdot\varrho(x,y,z)|_{z=Zp(x,y)}\right) + \nu\cdot\triangle V_x \\ \frac{\partial V_y}{\partial t} + V_x\frac{\partial V_y}{\partial x} + V_y\frac{\partial V_y}{\partial y} + V_z\frac{\partial V_y}{\partial z} = -\frac{g}{\varrho}\cdot\left(\int_z^{Zp(x,y)}\frac{\partial\varrho(x,y,z)}{\partial y}\cdot\partial z + \frac{\partial Zp(x,y)}{\partial y}\cdot\varrho(x,y,z)|_{z=Zp(x,y)}\right) + \nu\cdot\triangle V_y \\ \frac{\partial Z_p}{\partial t} + V_x\cdot\frac{\partial Z_p}{\partial x} + V_y\cdot\frac{\partial Z_p}{\partial y} = V_z|_{z=Z_p} = -\int_{Z_g}^{Z_p}\left(\frac{\partial V_x}{\partial x} + \frac{\partial V_y}{\partial y}\right)\partial z \\ \frac{\partial T}{\partial t} + V_x\cdot\frac{\partial T}{\partial x} + V_y\cdot\frac{\partial T}{\partial y} + V_z\cdot\frac{\partial T}{\partial z} = a\cdot(\triangle T) \\ \varrho = \Phi(T) \end{cases} \quad (7)$$

The evolution equation for determining the surface Z_p allows us to solve the system (7) by the establishment method, applying easy and comprehensible calculation algorithms and a well-developed tool of finite-difference schemes. However, when solving the system of equations (7), there are also difficulties that are difficult to eliminate.

Considering together the first, second and third equations of the system (7), we note that the group of these three equations describes the propagation of waves on the surface Z_p. The velocity of wave motion on the surface Z_p will be equal to the square root of the product of the acceleration of free fall by the depth of the flow of the moving medium under the surface Z_p. This velocity will be the main constraint for choosing the maximum possible time step. Convective motions of the medium slower than the wave velocity at the Z_p surface will be strongly smoothed by the action of the scheme viscosity. The consequence will be low informativeness of the obtained approximate solutions. Specialists working in the field of computational hydromechanics apply artificial heuristic digital constructions in the task of which is the destruction or reduction of high-speed waves on the surface Z_p preserving the possibility of smooth changes in the position of the surface Z_p.

A slightly different method of destroying surface waves is proposed. This method is not artificial. The method is based on the obvious fact that in a stable and unchanging solution, the surface must be stable as well.

That is, the value of $V_z|_{z=Z_p}$ must be equal to zero. Therefore, instead of a closed system of equations (7), assuming the presence of a single solution, it is proposed to solve a non-closed optimisation problem in which from the set of surface locations the one at which the value of $V_z|_{z=Z_p}$ will be minimal will be chosen. That is, it is proposed to solve the system of equations (8):

$$\begin{cases} \frac{\partial V_x}{\partial t} + V_x\frac{\partial V_x}{\partial x} + V_y\frac{\partial V_x}{\partial y} + V_z\frac{\partial V_x}{\partial z} = -\frac{g}{\varrho}\cdot\left(\int_z^{Zp(x,y)}\frac{\partial\varrho(x,z)}{\partial x}\cdot\partial z + \frac{\partial Zp(x,y)}{\partial x}\cdot\varrho(x,y,z)|_{z=Zp(x,y)}\right) + \nu\cdot\triangle V_x \\ \frac{\partial V_y}{\partial t} + V_x\frac{\partial V_y}{\partial x} + V_y\frac{\partial V_y}{\partial y} + V_z\frac{\partial V_y}{\partial z} = -\frac{g}{\varrho}\cdot\left(\int_z^{Zp(x,y)}\frac{\partial\varrho(x,y,z)}{\partial y}\cdot\partial z + \frac{\partial Zp(x,y)}{\partial y}\cdot\varrho(x,y,z)|_{z=Zp(x,y)}\right) + \nu\cdot\triangle V_y \\ V_z|_{z=Z_p} = -\int_{Z_g}^{Z_p}\left(\frac{\partial V_x}{\partial x} + \frac{\partial V_y}{\partial y}\right)\partial z \\ \frac{\partial T}{\partial t} + V_x\cdot\frac{\partial T}{\partial x} + V_y\cdot\frac{\partial T}{\partial y} + V_z\cdot\frac{\partial T}{\partial z} = a\cdot(\triangle T) \\ \varrho = \Phi(T) \\ OBJ = \int\left(V_z|_{z=Z_p}\right)^2 \to min \end{cases} \quad (8)$$

Where OBJ is the objective function of in the optimization problem.

The integration in the equation determining the objective function is performed over the entire Z_p surface, and the optimization problem is solved for each time step in the evolution of the heat transfer process T in the velocity field V_x, V_y, V_z. To verify the developed approach and demonstrate its ability to determine the convective transport of reserves, several test problems were solved.

The first test problem involved a pool of water, a weakly compressible liquid, subjected to non-uniform heating. The following conditions were assumed: the water surface on the right side of the basin was cooled to a temperature of 4 degrees Celsius (the temperature of maximum water density), while on the left side, the water surface was heated to 30 degrees Celsius. The spatial steps were set to 1 meter. The evolution equations of system (8) were approximated by explicit schemes, with the explicit scheme (Salokhiddinov et al., 2022a; Salokhiddinov et al., 2022b; Salokhiddinov et al., 2023) being employed due to its capability to fully execute conservation laws across all possible configurations of the velocity vector field. The establishment method was utilized to solve the problem, and at each step of the solution evolution, an optimization problem was solved to determine the equilibrium position of the free surface of the moving water.

The selection of the topic of heat transfer in liquids is justified by the fact that problems of heat transfer in air and water are sufficiently similar to justify a unified approach. The findings of the study indicate that hydrodynamic heat transfer models developed for water content systems can be verified and effectively applied to air content systems. The high degree of accuracy demonstrated by CFD models in predicting heat and mass transfer, coupled with the successful empirical validation and sensitivity analyses conducted, confirm their applicability in a range of scenarios. Consequently, the analogous solutions obtained from examining heat transfer in both air and water can be employed for model validation (Kondjoyan et al., 2006; Talukdar et al., 2008; Sadafi et al., 2015; Tingfen et al., 2019).

The second test problem pertains to the primary objective of this paper, namely, the modeling of the formation of thermal islands in an arbitrary and complex configuration of the landform surrounding the calculation area. The ensuing conditions are stipulated as follows: two adjacent structures (high and low) are considered, with both structures situated on the right receiving radiant energy from the sun. In lieu of meticulously tracking the precise position and algorithmization of boundary conditions on the surfaces of impermeable objects within the calculation domain, it is proposed to subtract from the right side of the horizontal component of the equation of motion the product of the velocity by a coefficient that is significantly greater than one. Theoretically, this would allow air flow to pass through obstacles while simultaneously experiencing a significant braking effect from the obstacles. When the coefficient is set to a value of 100, the airflow's progression through obstacles becomes virtually halted. This heuristic approach facilitates the incorporation of obstacles of the most intricate and impermeable nature into the calculation algorithm, thereby ensuring their comprehensive consideration.

The medium of movement is air; the solution has been carried out by analogy with the analysis of fluid motion in Problem 1. The initial average air temperature was assumed to be 30°C, and this value was held constant over the entire area of study. Spatial steps were taken equal to 1 meter. The system of equations (8) was utilized to solve this rather complex hydrodynamic problem.

The computations and the construction of the plots were carried out using programs written by the authors in the GAMS (General Algebraic Modeling System) programming language.

RESULTS & DISCUSSION

Results of solving the test problem 1. In order to obtain the stationary solution to the initial problem, a total of 200 iterations were performed. The calculation grid comprised 36 nodes in the horizontal direction and 60 nodes in the vertical direction. The graphical representation of the solution to the problem is depicted in Fig. 1. This Fig. illustrates the anticipated circular motion of the water in the vertical plane (longitudinal section of the pool) resulting from the uneven heating of the free surface.

This number of iterations was sufficient to form a stationary field of temperatures and density. Based on this stationary field of density, a stationary field of motion velocities was also formed.

Fig. 2 shows the profile of the free surface of the water in the pool. A salient feature pertains to the absence of wave processes on the free surface and the precise fulfillment of the water balance on any vertical plane within the circular motion region. The accuracy of the water balance is ensured by the condition that the vertical component of the water velocity at the height of the free surface is equal to zero.

As illustrated in Fig. 3, the horizontal velocity of water in relation to the vertical at the center of the basin is examined. It is observed that the flow of water in the pool from left to right and from right to left is identical. This exact equality is also noted for all verticals. This equality is observed at each step of the evolutionary search for velocity and temperature fields. The duration of the optimization at each evolutionary step is approximately one second for a given number of nodes in the computational domain.

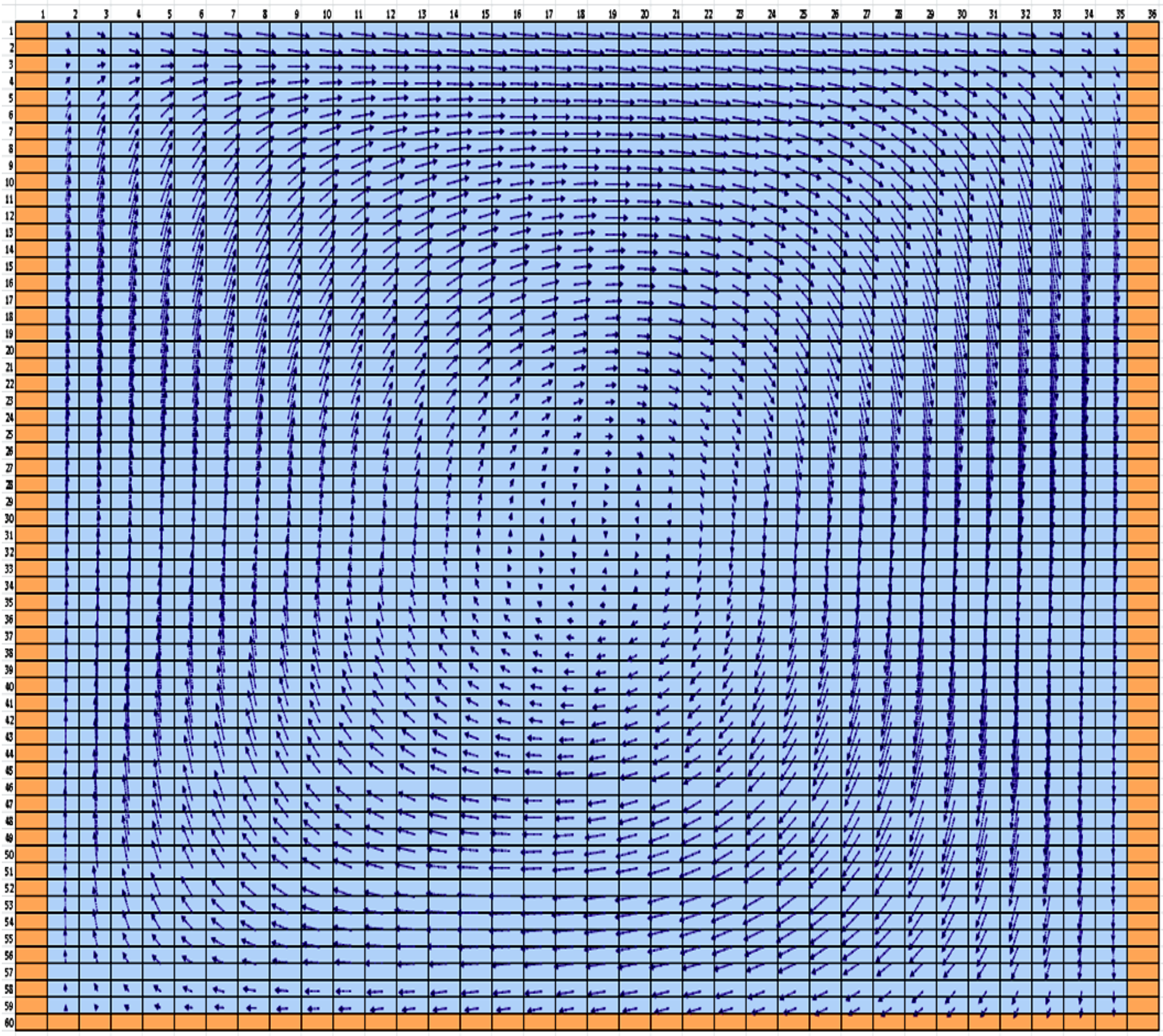

Fig. 1: Circular motion generated in the vertical plane in the pool by uneven heating of the free water surface in the pool.

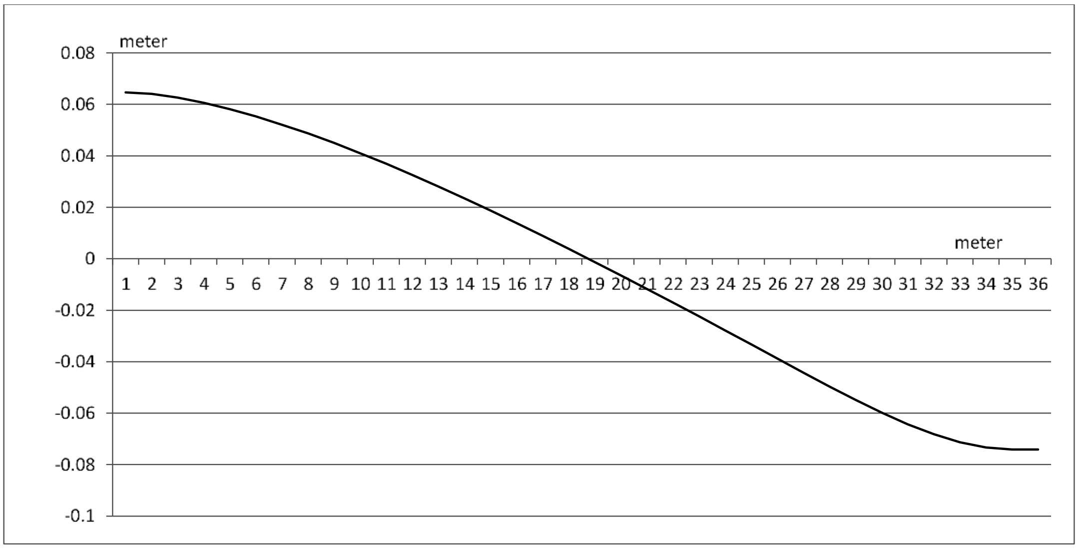

Fig. 2: Profile of the free surface of the water in the basin.

It is noteworthy that the precise equality of the water balance, as demonstrated in the solution to system (7), is attainable only at the nascent stages of the solution's evolution in conventional evolutionary computations of the position of the free surface.

Results of the solution of the test problem 2. The ensuing discussion will focus on the results of the solution to problem 2, which pertains to the formation of thermal islands in an arbitrary and complex configuration of the relief shape surrounding the calculation area. The graphical results of the solution are presented in Fig. 4, which illustrates the velocity field of the air involved in convective mixing in the presence of two buildings in the computational domain.

It is assumed that the right side of the building faces the sun and is heated four degrees Celsius more than the left side of the building. The average temperature of the air mixture entering the computational domain is assumed to be 30 degrees Celsius. A strong updraft is clearly visible on the right side of the domain and near the eastern building. The airflow quickly rises along the side of the building facing the sun. In addition, the airflow is pressed against the surface of the building as much as possible. On the non-sunny side of the tall building, there is a slight decrease in airflow. Most likely, this is a compensatory flow from the updraft on the sunny side of the low building further to the left. The lower building on the left side of the calculation area did not develop strong ascending air currents. The height of the lower task was not high enough to generate significant updrafts.

The second test problem was solved under the condition of free passage of the air mass through its left and right edges. Calculations have shown that with such an arrangement of buildings there is a shift of the entire airflow to the right. This means that not only local circulation currents occur, but also a general transfer of air from left to right. The heat from sunlight emitted on the right side of a tall building, which rises upwards, leaves the computational domain mainly through its right edge. There is a horizontal absorption of the entire air mass surrounding both the low and high buildings. A numerical experiment has shown that skyscrapers are not only able to change air currents locally, but also to shape them at considerable distances.

It is imperative to acknowledge and underscore the efficacy of the heuristic approach in accounting for obstacles within the calculation zone. The air flow velocities calculated within the confines of these obstacles are found to be negligible. This outcome indicates that the impact of obstacles on airflow is not achieved through the construction of boundary conditions within the solution area. Instead, it is accomplished by assigning forces of resistance to the movement of the flow by buildings - obstacles.

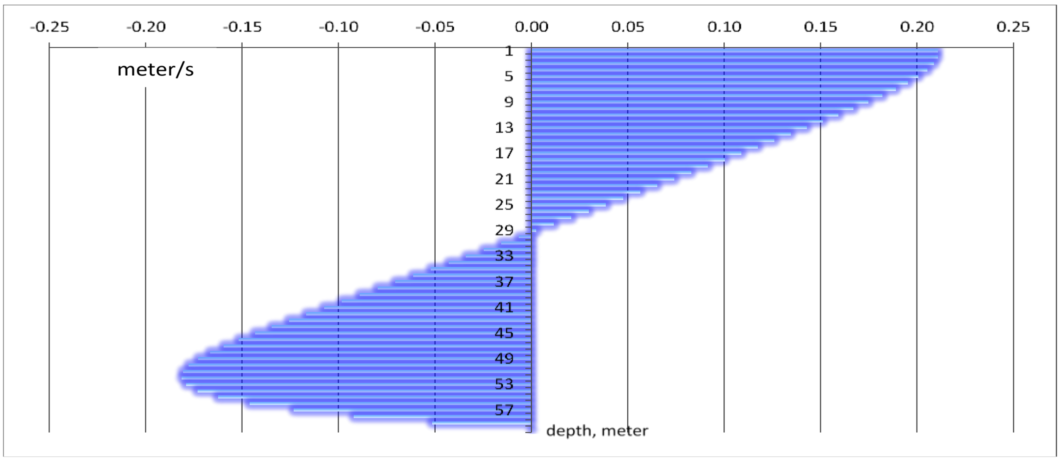

Fig. 3: The horizontal water velocity diagram on the vertical at the center of the basin.

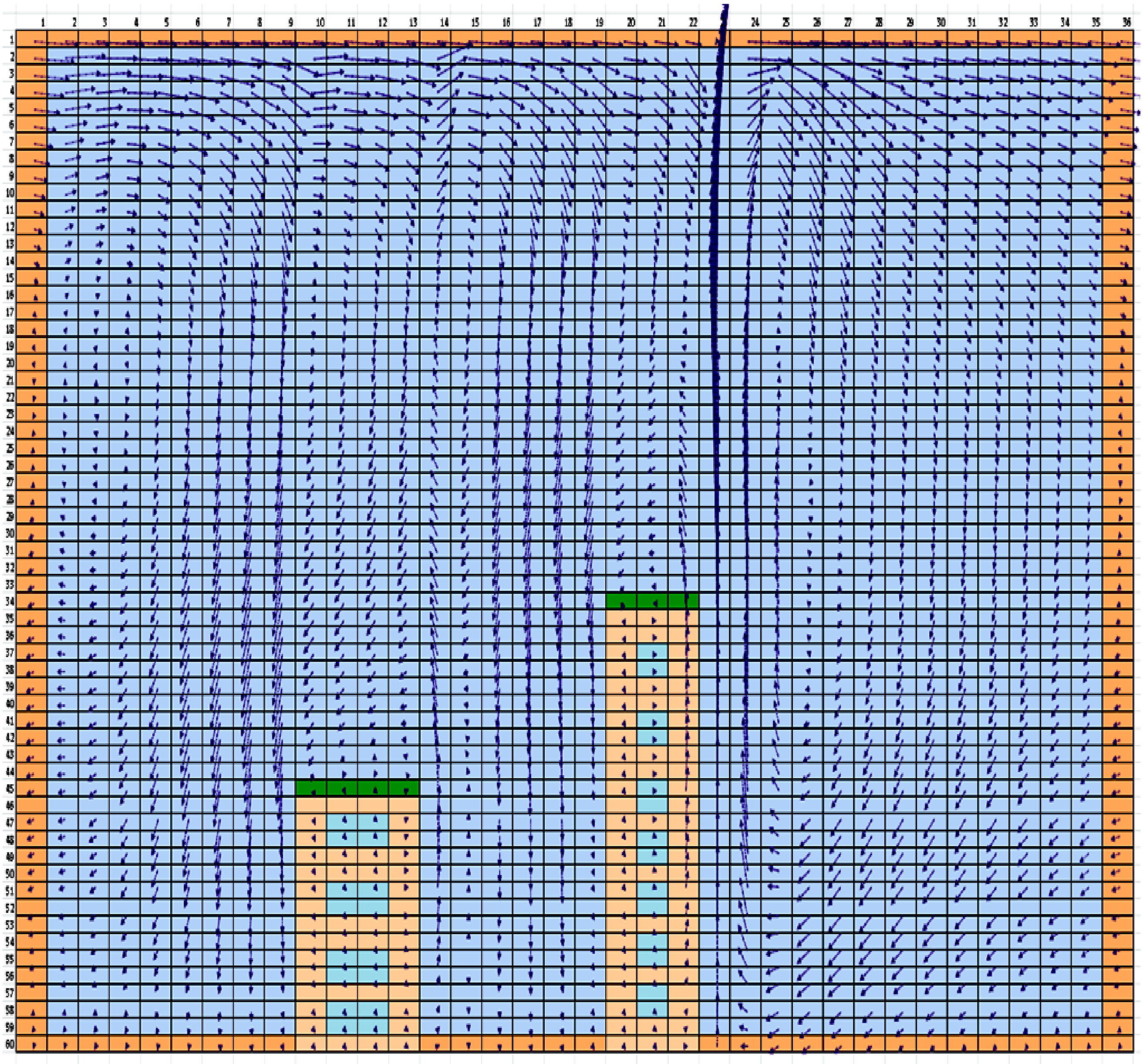

Fig. 4: The field of air velocities surrounding buildings that are heated by sunlight from the right side.

Fig. 5 illustrates the temperature field's deviation from the mean value. The calculation indicates that due to the heating of the right side of the buildings, the temperature has increased to an average of 32 degrees Celsius. The color scale, presented in five shades, is located in 20 percent increments from the minimum to the maximum temperature deviation from the average value (assumed to be 32 degrees). More intense colors correspond to higher temperatures. The findings offer a comprehensive representation of air mass microcirculation and heat transfer in urban environments, paving the way for large-scale urban microclimate modeling. As illustrated in Fig. 5, the maximum temperatures are observed to be concentrated within the buildings, aligning with the results reported by other researchers (Minh and Nguyen, 2019; Minh & Shukurov, 2020).

Further analysis of both test problems reveals strong alignment with previous research on convective flows and heat transfer dynamics in various environmental conditions. For Problem 1, the observed absence of wave processes on the free water surface, as shown in Fig. 2, corroborates findings from prior simulations and experimental setups analyzing stationary fluid dynamics with distinct thermal gradients. The precise equality of water balance demonstrated in our calculations validates the methodological approach and strengthens the reliability of the numerical models. The results of Problem 2, particularly the air velocity field patterns shown in Fig. 4 and temperature deviations illustrated in Fig. 5, demonstrate the occurrence of localized thermal island effects around heated structures. The observed distinct upward and lateral flows align with significant air circulation patterns influenced by urban morphology and heating intensities (Fan et al., 2019). Our findings regarding thermal buildup on the non-sunny sides of buildings echo previous research showing that heat dissipation efficiencies vary depending on the aspect ratio and geometric configuration of urban structures.

The thermal deviations from average values observed in our second test problem are consistent with heat flux studies by Kahsay et al. (2019), which highlight how

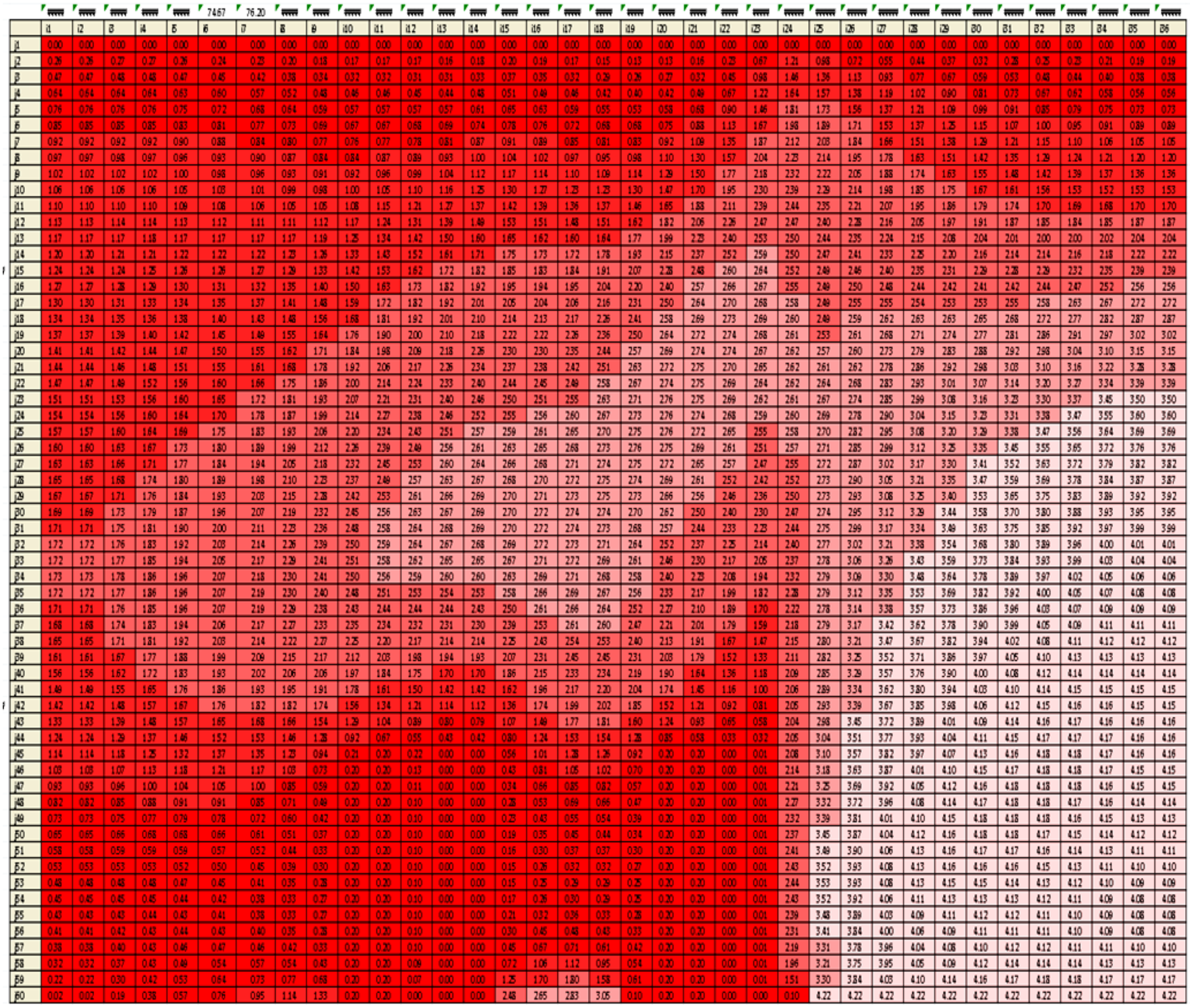

Fig. 5: Field of air temperature deviations from the mean value due to convective transport caused by uneven heating of the buildings by the sunlight.

uneven heating leads to nuanced variations in convective .heat transfer coefficients (CHTC) across facade surfaces. This is particularly evident in our observations of upward flow dynamics near heated regions, underscoring the significance of vertical temperature gradients in driving localized microcirculations. The findings of Anbarsooz et al. (2022) provide further support for these observations, particularly in their analysis of heat transfer coefficients at building facades in different configurations. Our implementation of the heuristic approach to describing obstacles in airflow, combined with the optimization method, addresses some of the uncertainties discussed by Mirsadeghi et al. (2013) regarding external heat transfer coefficient modeling. While our study utilizes reliable numerical approximations, we acknowledge that external variables, such as building geometry and environmental factors, can introduce variances in urban thermal modeling. This understanding is crucial for the accurate interpretation and application of our results.

The practical implications of our findings for urban planning and design are significant, particularly in the context of the observed thermal island formation and air circulation patterns. These findings align with Battista (2017), who advocate for the integration of computational models in planning processes to enhance the prediction of heat flow dynamics in urban canyons. The work of Vollaro et al. (2015) further supports our approach, particularly their CFD analysis of convective heat transfer coefficients on external building surfaces. The successful application of our optimization-based method and heuristic approach to obstacle representation demonstrates the potential for efficient modeling of complex urban thermal dynamics.

Conclusion

Problems of this type are usually solved approximately by finding a stationary solution in evolutionary equations. This method requires a very large number of iterations and contains manifestations of wave processes in the solutions. Strong restrictions on time steps in iterations appear and the solution process takes a significant amount of time. The proposed method for the approximate solution of hydrodynamic and aerodynamic problems, consisting in the combination of the evolutionary approach and the optimization of a number of variables in the process of their search at each iterative step, allowed: to obtain the solution quickly and to achieve the exact fulfillment of the laws of conservation of mass of the moving medium and the complete absence of wave phenomena, which are not of interest for this type of problems. A new finite difference scheme (Salokhiddinov et al., 2022a; Salokhiddinov et al., 2022b; Salokhiddinov et al., 2023) was used to determine the transport of matter, momentum and heat energy in solving the problem. This scheme ensures the exact fulfillment of the conservation laws of matter, momentum and thermal energy for any configuration of velocity fields.

A heuristic approach to describing obstacles in the path of air flow has been tested and shown to be effective. This study contributes to the understanding of convective heat transfer in urban settings by providing both methodological advances and practical insights. The combination of our optimization approach with the heuristic treatment of obstacles offers an efficient way to model complex urban geometries while maintaining solution accuracy. These findings not only validate existing research but also provide new insights into the complex dynamics of urban heat transfer, particularly in the context of modern architectural configurations and urban densification. Subsequent research endeavors should prioritize the extensive validation of the obtained results on the scale of high-rise city development, leveraging micrometeorological stations. The findings will be instrumental in formulating measures aimed at enhancing the thermal comfort of urban streets.

Author's Contribution: All authors contributed equally in this research. Authors have no conflict of interest.

REFERENCES

Anbarsooz, M., Mirian, H. & Ahmadi, G. (2022). Numerical analysis of convective heat transfer coefficients at the facades of two cubical buildings in tandem and staggered configurations. *Heat Mass Transfer*, 58, 1979–1996. https://doi.org/10.1007/s00231-022-03226-x

Anderson, D., Tannehill, J., & Pletcher, R. (1990). Computational hydromechanics and heat exchange. Mir Publications, Moscow, Russia.

Awol, A., Bitsuamlak, G., & Tariku, F. (2020). Numerical estimation of the external convective heat transfer coefficient for buildings in an urban-like setting. *Building and Environment*, 169, 106557. https://doi.org/10.1016/j.buildenv.2019.106557

Battista, G. (2017). Analysis of Convective Heat Transfer at Building Facades in Street Canyons. *Energy Procedia*, 113, 166-173. doi 10.1016/j.egypro.2017.04.048

Batchelor, J., & Moffat, G. (1984). Modern hydrodynamics. Advances and problems. *Journal of Fluid Mechanics*, 140, 48-61.

Blocken, B., Stathopoulos, T., Carmeliet, J., & Hensen, J. (2011). Application of computational fluid dynamics in building performance simulation for the outdoor environment: An overview. *Journal of Building Performance Simulation*, 4(2), 157-184. https://doi.org/10.1080/19401493.2010.513740

Chung, J.D., & Choo, M.-L. (2011). Computational fluid dynamics for urban design: The prospects for greater integration. *International Journal of Architectural Computing*, 9(1), 33-54. https://doi.org/10.1260/1478-0771.9.1.33

Donthu, E.K.K., Shashwat, S., Zingre, K.T., & Wan, M.P. (2024). Development of a simplified cool coating thermal model for predicting street canyon air temperature. *Building and Environment*, *251*, 111207. https://doi.org/10.1016/j.buildenv.2024.111207

Irfeey, A., Chau, H., Sumaiya, M., Wai, C., Muttil, N., & Jamei, E. (2023). Sustainable mitigation strategies for urban heat island effects in urban areas. *Sustainability*. https://doi.org/10.3390/su151410767

Ismael, S., Alias, A., Haron, N., Bahaa, B., & Abdulghani, A. (2024). Mitigating urban heat island effects: A review of innovative pavement technologies and integrated solutions. *Structural Durability & Health Monitoring*, 18, 1-10. https://doi.org/10.32604/sdhm.2024.050088

Fan, Y., Wang, Q., Yin, S., & Li, Y. (2019). Effect of city shape on urban wind patterns and convective heat transfer in calm and stable background conditions. *Building and Environment*, *162*, 106288. https://doi.org/10.1016/J.BUILDENV.2019.106288

Furukawa, K., Giga, Y., & Kashiwabara, T. (2020). The hydrostatic approximation for the primitive equations by the scaled Navier–Stokes equations under the no-slip boundary condition. *Journal of Evolution Equations*, 21, 3331-3373. https://doi.org/10.1007/s00028-021-00674-6

Gagliano, A., Detommaso, M., Nocera, F., Patania, F., & Aneli, S. (2014). The retrofit of existing buildings through the exploitation of the green roofs: A simulation study. *Energy Procedia*, 62, 52-61. https://doi.org/10.1016/j.egypro.2014.12.366

Gago, E.J., Roldan, J., Pacheco-Torres, R., & Ordóñez, J. (2013). The city and urban heat islands: A review of strategies to mitigate adverse effects. *Renewable and Sustainable Energy Reviews*, 25, 749-758. https://doi.org/10.1016/j.rser.2013.05.057

Gao, H., Nečasová, Š., & Tang, T. (2021). On the hydrostatic approximation of compressible anisotropic Navier–Stokes equations. *Comptes Rendus. Mathématique*, *359*(6), 639-644. https://doi.org/10.5802/crmath.186

Haddad, L., Aouachria, Z., & Haddad, D. (2015). Impact of the transport on the urban heat island. *International Journal for Traffic and Transport Engineering*, 5(3), 252-263. https://doi.org/10.7708/ijtte.2015.5(3).03

Jia, S., Wang, Y., Wong, N. H., & Weng, Q. (2025). A hybrid framework for assessing outdoor thermal comfort in large-scale urban environments. *Landscape and Urban Planning*, *256*, 105281. https://doi.org/10.1016/j.landurbplan.2024.105281

Kahsay, M.T., Bitsuamlak, G., & Tariku, F. (2019). Numerical analysis of convective heat transfer coefficient for building facades. *Journal of Building Physics*, *42*(6), 727-749. DOI: 10.1177/1744259118791207

Kondjoyan, A., Rouaud, O., Mccann, M., Havet, M., Foster, A., Swain, M., & Daudin, J. (2006). Modelling coupled heat–water transfers during a decontamination treatment of the surface of solid food products by a jet of hot air. *Journal of Food Engineering*, 76, 53-62. https://doi.org/10.1016/J.JFOODENG.2005.05.014

Lax, P.D., & Richtmyer, R.D. (1956). Survey of the stability of linear finite difference equations. *Communications on Pure and Applied Mathematics,* 9(2), 267–293.

Liu, J., Heidarinejad, M., Gracik, S., Srebric, J., & Yu, N. (2015). An indirect validation of convective heat transfer coefficients (CHTCs) for external building surfaces in an actual urban environment. *Building Simulation*, 8, 337-352. https://doi.org/10.1007/S12273-015-0212-0

Luo, X., Hong, T., & Tang, Y.H. (2020). Modeling thermal interactions between buildings in an urban context. *Energies*, *13*(9), 2382. https://doi.org/10.3390/en13092382

Marchuk, G.I., Kordzadze, A.A., & Skiboy, Y.N. (1975). Calculation of main hydrological fields of the Black Sea. *Proceedings of the USSR Academy of Sciences, Series Physics of the Atmosphere and Ocean*, 11(4), 370-393.

Marchuk, G.I., & Kurbatkin, G.P. (1978). *Numerical weather forecasting of Earth and Universe*, 28, 37-43

Marchuk, G.I. (1980). *Mathematical models of circulation in the ocean*. Nauka, Novosibirsk.

Memon, R.A., Leung, D.Y.C., & Chunh, L. (2008). A review on the generation, determination, and mitigation of urban heat island. *Journal of Environmental Sciences*, 20, 120-128. https://doi.org/10.1016/S1001-0742(08)60019-4

Mehrotra, S., Bardhan, R., & Ramamritham, K. (2020). Diurnal thermal diversity in heterogeneous built area: Mumbai, India. *Urban Climate*, *32*, 100627. https://doi.org/10.1016/j.uclim.2020.100627

Minh, T.L., & Nguyen, A.Q.T. (2019). Features of the formation of urban heat islands effects in tropical climates and their impact on the ecology of the city. *E3S Web of Conferences*, 91, 05005. https://doi.org/10.1051/e3sconf/20199105005

Minh, T.L., & Shukurov, I. (2020). Modelling of the heat-wind regime of the urban street in Hanoi. *Vestnik of MSCU*, *15*(3), 368-379.

Mirsadeghi, M., Cóstola, D., Blocken, B., & Hensen, J. (2013). Review of external convective heat transfer coefficient models in building energy simulation programs: Implementation and uncertainty. *Applied Thermal Engineering*, 56, 134–151. https://doi.org/10.1016/j.applthermaleng.2013.03.003

Moediartianto, A., Montazeri, H., & Blocken, B. (2018). Numerical and wind-tunnel analysis of convective heat transfer at ground surfaces around complex building models. *Paper presented at the 8th International Conference on Environmental Effects on Buildings and People: Actions, Influences, Interactions, Discomfort (EEBP VIII)*, Cracow, Poland.

Mohajer, H., Ding, L., Kolokotsa, D., & Santamouris, M. (2023). On the Thermal Environmental Quality of typical urban settlement configurations. *Buildings*, *13*(1), 76. https://doi.org/10.3390/buildings13010076

Nekkanti, H., & Radhakrishnan, N. (2024). Analysis of Rivers' Hidden Cooling Potential on a River Front City-a Case Study on Vijayawada City, Andhra Pradesh, India. *Journal of the Institution of Engineers (India): Series A*, 10, 1-11. https://doi.org/10.1007/s40030-024-00843-z

Nottrott, A., Onomura, S., Inagaki, A., Kanda, M., & Kleissl, J. (2011). Convective heat transfer on leeward building walls in an urban environment: Measurements in an outdoor scale model. *International Journal of Heat and Mass Transfer*, 54(16), 3128-3138. https://doi.org/10.1016/J.IJHEATMASSTRANSFER.2011.04.020

Oke, T.R. (1982). The energetic basis of the urban heat island. *Quarterly Journal of the Royal Meteorological Society*, 108, 1-24. https://doi.org/10.1002/qj.49710845502

Panwar, M., & Jindal, S., (2024). Urban Heat Island and Building Energy Consumption. *IOP Conference Series: Earth and Environmental Science*, 1326, 012080. https://doi.org/10.1088/1755-1315/1326/1/012080

Ricardo, K., Lee, D., & Duru, K. (2024). Entropy and energy conservation for thermal atmospheric dynamics using mixed compatible finite elements. *Journal of Computational Physics*, *496*, 112605. https://doi.org/10.1016/j.jcp.2023.112605

Roache, P.J. (1976). Computational fluid dynamics Hermosa. *Albuquerque, NM*, 28, 140-149.

Sadafi, M., Jahn, I., Stilgoe, A., & Hooman, K. (2015). A theoretical model with experimental verification for heat and mass transfer of saline water droplets. *International Journal of Heat and Mass Transfer*, 81, 1-9. https://doi.org/10.1016/J.IJHEATMASSTRANSFER.2014.10.005

Salokhiddinov, A., Savitsky, A., McKinney, D., & Ashirova, O.A. (2022a). An improved finite-difference scheme for the conservation equations of matter. *Proceedings of Annual International Scientific Conferences: GIS in Central Asia – GISCA 2022 and Geoinformatics – GI 2022*, E3S Web of Conferences, 386, 06002. https://doi.org/10.1051/e3sconf/202338606002

Salokhiddinov, A., Savitsky, A., & Ashirova, O. (2022b). Research of conservative finite-difference scheme for transfer equations. *Journal of Irrigation and Melioration*, 1 (27), 13-17.

Salokhiddinov, A., Savitsky, A., Radkevich, M., & Ashirova, O. (2023). Possibilities of solving two-dimensional hydrodynamic problems on the basis of the non-divergent form of recording the transport and conservation equations. *E3S Web Conf.*, 434, 01001. https://doi.org/10.1051/e3sconf/202343401001

Santamouris, M. (2014). Cooling the cities—A review of reflective and green roof mitigation technologies to fight heat island and improve comfort in urban environments. *Solar Energy*, 3, 682-703. https://doi.org/10.1016/j.solener.2012.07.003

Schrijvers, P.J.C., Jonker, H.J.J., Kenjere, S., & Roode, S.R.de. (2018). Breakdown of the nighttime urban heat island energy budget. *Building and Environment*, 83, 50-64. https://doi.org/10.1016/j.buildenv.2014.08.012

Talukdar, P., Iskra, C., & Simonson, C. (2008). Combined heat and mass transfer for laminar flow of moist air in a 3D rectangular duct: CFD simulation and validation with experimental data. *International Journal of Heat and Mass Transfer*, 51, 3091-3102. https://doi.org/10.1016/J.IJHEATMASSTRANSFER.2007.08.034

Tingfen, K., Huang, X., & Ling, X. (2019). Numerical and experimental analysis on air/water direct contact heat and mass transfer in the humidifier. *Applied Thermal Engineering*, *156*, 310-323 https://doi.org/10.1016/J.APPLTHERMALENG.2019.04.051

Turhan, C., Atalay, A.S., & Gokcen Akkurt, G. (2023). An integrated decision-making framework for mitigating the impact of urban heat islands on energy consumption and thermal comfort of residential buildings. *Sustainability*, *15*(12), 9674. https://doi.org/10.3390/su15129674

Vollaro, A.de L., Galli, G., & Vallati, A. (2015). CFD Analysis of Convective Heat Transfer Coefficient on External Surfaces of Buildings. *Sustainability*, 7, 9088-9099. doi:10.3390/su7079088

Wei, R., Tsai, Y., & Chen, S. (2021). Improved Schemes of Differential Spatial Modulation. *IEEE Access*, 9, 97120-97128. https://doi.org/10.1109/ACCESS.2021.3095531

Yuan, F., & Bauer, M.E. (2007). Comparison of impervious surface area and normalized difference vegetation index as indicators of surface urban heat island effects in Landsat imagery. *Remote Sensing of Environment*, 106(3), 375-386. https://doi.org/10.1016/j.rse.2006.09. 003